Journal of Medicinal Chemistry Article

J. Med. Chem. **2010,** *53,* 8747–8759 **8747**
DOI: 10.1021/jm1009988

Structure-Based Design, Synthesis, and Pharmacological Evaluation of 3-(Aminoalkyl)-5-fluoroindoles as Myeloperoxidase Inhibitors†

Jalal Soubhye,[‡] Martine Prévost,[§] Pierre Van Antwerpen,[‡,∥] Karim Zouaoui Boudjeltia,[⊥] Alexandre Rousseau,[⊥] Paul G. Furtmüller,[#] Christian Obinger,[#] Michel Vanhaeverbeek,[⊥] Jean Ducobu,[⊥] Jean Nève,[‡] Michel Gelbcke,[‡] and François Dufrasne*[,‡]

[‡]*Laboratoire de Chimie Pharmaceutique Organique, Faculté de Pharmacie, Université Libre de Bruxelles, Brussels, Belgium,* [§]*Laboratoire de Structure et Fonction des Membranes Biologiques, Université Libre de Bruxelles, Brussels, Belgium,* [∥]*Analytical Platform of the Faculty of Pharmacy, Université Libre de Bruxelles, Brussels, Belgium,* [⊥]*Laboratory of Experimental Medicine, CHU Charleroi, A. Vésale Hospital, Université Libre de Bruxelles, Montigny-le-Tilleul, Belgium, and* [#]*Department of Chemistry, Division of Biochemistry, BOKU—University of Natural Resources and Life Sciences, Vienna, Austria*

Received June 15, 2010

Oxidized low-density lipoproteins (LDLs) accumulate in the vascular wall and promote local inflammation, which contributes to the progression of the atheromatous plaque. The key role of myeloperoxidase (MPO) in this process is related to its ability to modify APO B-100 in the intima and at the surface of endothelial cells. A series of 3-(aminoalkyl)-5-fluoroindole analogues was designed and synthesized by exploiting the structure-based docking of 5-fluorotryptamine, a known MPO inhibitor. In vitro assays were used to study the effects of these compounds on the inhibition of MPO-mediated taurine chlorination and oxidation of LDLs. The kinetics of the interaction between the MPO redox intermediates, Compounds I and II, and these inhibitors was also investigated. The most potent molecules possessed a 4- or 5-carbon aminoalkyl side chain and no substituent on the amino group. The mode of binding of these analogues and the mechanism of inhibition is discussed with respect to the structure of MPO and its halogenation and peroxidase cycles.

Introduction

The heme enzyme, myeloperoxidase (EC 1.11.1.7, MPO[a]), is one of the key players in the first line of the nonspecific immune defense system.[1] In the presence of hydrogen peroxide and halide ions, MPO catalyzes the synthesis of hypohalous acids (e.g., hypochlorous acid, HOCl). These oxidizing and halogenating compounds kill and destruct foreign microorganisms. MPO is packed in the azurophilic granules of (phagocytosing) polymorphonuclear leukocytes in relatively high concentrations (typically up to 5% of cell dry weight) and is released into the phagosomes that contain the endocytosed pathogens. However, MPO can also be released outside the phagocytes[1] and contribute to tissue damage at sites of inflammation. In addition to its beneficial role in microbial killing, MPO is reported to be involved in a growing number of diseases because of its ability to generate reaction products that can oxidize many types of biomolecule (lipids, proteins, DNA, etc.).

MPO can influence disease pathogenesis in two ways: In the first, MPO is directly involved at the origin of the disease;[2,3] in the second, MPO acts to worsen symptoms associated with inflammatory conditions.[4−10] Several of these pathologies present major problems for public health at a global level. To investigate the involvement of MPO in cardiovascular disease, we focused our attention on atherosclerosis. It is well-known that MPO oxidizes the apolipoprotein (APO) B-100 of low-density lipoproteins (LDLs), thereby contributing to the development of atherosclerosis.[11] Indeed, LDLs oxidized by MPO (Mox-LDL) can induce foam cell formation and trigger inflammatory responses in monocytes and endothelial cells.[1,12] The interaction between MPO and LDL is facilitated by electrostatic interactions as MPO is strongly basic[1] at physiological pH, whereas LDLs are negatively charged. In addition, it has been shown that MPO can oxidize the APO A1 of high-density lipoproteins (HDLs), thus impairing reverse cholesterol transport.[13,14] Because of these deleterious effects, development of therapeutic strategies aimed at inhibiting MPO is needed.[15] However, despite several attempts, there are still no molecules with sufficient in vitro and/or in vivo inhibiting properties.[16−28]

We recently assessed the MPO inhibiting effects of commonly used anti-inflammatory drugs.[29] Flufenamic acid (**1**, Figure 1) was identified as a good candidate, which inhibited both HOCl production and LDL oxidation.[29] However, these results were only observed at high concentrations, rendering flufenamic acid unusable because of its toxic adverse effects at these doses. Analogous compounds were also investigated but none had better inhibitory activity,[16] likely because their negative charge dampened the interaction between MPO and anionic LDLs.[30] We, therefore, hypothesized that positively

†The PDB code of MPO is 1DNW.

*To whom correspondence should be addressed. Phone: 003226505235. Fax: 003226505249. E-mail: dufrasne@ulb.ac.be. Address: Campus plaine, CP 205/5, 1050 Brussels, Belgium.

[a] Abbreviations: APO B-100, apolipoprotein; DIBAL-H, diisobutylaluminium hydride; DMA, dimethylacetamide; DMSO, dimethylsulfoxide; EtOAc, ethyl acetate; EtOH, ethanol; LDL, low-density lipoprotein; MPO, myeloperoxidase; TEA, triethylamine.

Published on Web 11/22/2010

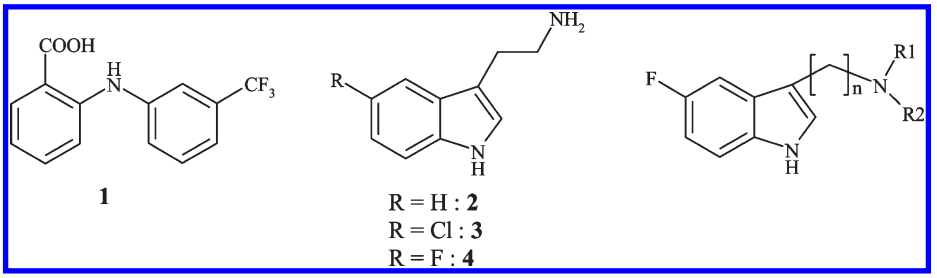

Figure 1. General structure of flufenamic acid (**1**), tryptamine derivatives (**2**,**3**,**4**), and 5-fluoroindole-3-alkylamine derivatives (**3**).

charged compounds could overcome this problem and in addition would allow more favorable interactions with anionic amino acid residues at the active site of MPO.

Jantschko et al. (2005) showed that tryptamine (**2**) derivatives act as substrates and inhibitors of MPO. Derivatives that carry a metabolically stable substituent on position 5 of the indole ring, such as chlorine (5-chlorotryptamine, **3**) or fluorine (5-fluorotryptamine, **4**), were shown to be efficient reversible inhibitors.[31] It must be noted that the stability of the aromatic moiety of potential inhibitors is crucial because the indole ring is subject to oxidation by MPO, particularly on position 5.[32] Substitution by electron-withdrawing groups makes the indole moiety very fragile and prone to cleavage between C-2 and C-3. This has been demonstrated with melatonin, which possesses an OMe group on position 5.[33,34] A promising MPO drug candidate must be a stable molecule and good substrate so that administered doses and the risk of adverse effects can be kept as small as possible.

By exploiting the positions of 5-fluorotryptamine obtained from structure-based docking, we designed analogues that could have additional interactions with the active site of the heme enzyme. Two strategies were followed, namely varying the length of the aminoalkyl side chain and adding substituents of different sizes to the amino group of the side chain. These analogues were then synthesized and their capacity to inhibit recombinant MPO, produced in CHO-cell lines, was measured. We report the effect of these new compounds on MPO-mediated taurine chlorination and LDL oxidation and on the interaction with the "Compound I" and "Compound II" redox intermediates of MPO. We also propose a mechanism for the inhibition.

Results

Docking Experiments. Indole and tryptamine derivatives have been reported to be reversible inhibitors of human MPO with 5-fluorotryptamine being the most effective.[31] These findings prompted us to perform a rational structure-based design of new tryptamine derivatives based on the docking of 5-fluorotryptamine. The reliability of the docking procedure was previously assessed by comparing the docking of salicylhydroxamic acid with its position in the crystal structure of the MPO complex.[16]

The best pose of 5-fluorotryptamine (Figure 2A) featured stacking of the indole 6-membered ring onto the pyrrole ring D of the heme. Stacking was also observed in the crystal structure of the MPO structure in complex with salicylhydroxamic acid. In addition to the stacking, one salt bridge was formed with Glu102 and one hydrogen bond with Thr100. No hydrogen bond was observed between the indole NH group and the protein. Another pose featured a hydrogen bond but at the expense of the stacking. Interestingly, empty pockets remained around the docked ligand and could

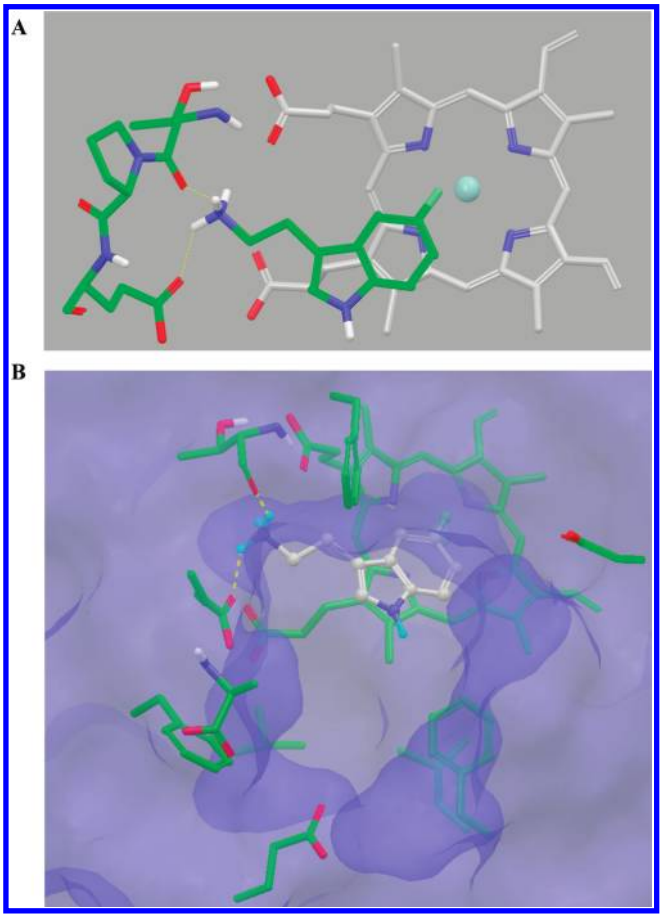

Figure 2. (A) Best pose of 5-fluorotryptamine (**4**) generated by the Glide docking program. The ligand is depicted as stick. Neighboring residues including Thr100 and Glu102, which hydrogen bond to the ligand and the heme (with carbon atoms in light gray), are also illustrated. The small blue sphere indicates the location of the ferric ion at the center of the heme. (B) View from the entrance of the channel of the best pose of 5-fluorotryptamine (**4**) with a representation of the molecular surface of the protein and neighboring hydrophobic, negatively charged residues and Thr100 (see text), which were accounted for design the 5-fluorotryptamine analogues.

be exploited to create structural modifications of 5-fluorotryptamine (Figure 2B). In particular, the voids facing Phe99, Phe147, Leu420, Phe407, and Leu406 could be filled with chemical groups so as to form additional hydrophobic interactions between the ligand and the binding site. On the basis of these observations, we developed two strategies for creating the analogues: (i) varying the length of the alkyl side chain and (ii) adding different alkyl or cyclic substituents on the side chain nitrogen. The amino group of 5-fluorotryptamine that bears a positive charge at physiological pH was conserved so as to keep the potential formation of an ionic

Table 1. IC_{50} Values for the Inhibition of MPO, Predicted Free Energies of Binding Obtained from Docking Experiments[a]

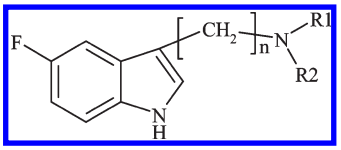

no.	*n*	R_1	R_2	IC_{50} (μM)	ΔG (kcal/mol)
6	1	H	H	0.9 ± 0.3	−5.3
7	1	C_2H_5	C_2H_5	0.2 ± 0.2	−6.3
8	1	*N*-methylpiperazinyl		1.0 ± 0.1	−7.3
4	2	H	H	0.20 ± 0.03	−6.5
16	2	CH_3	H	0.20 ± 0.02	−6.6
17	2	C_2H_5	H	0.3 ± 0.1	−6.8
18	2	C_3H_7	H	0.80 ± 0.02	−6.6
19	2	C_4H_9	H	1.03 ± 0.08	−6.5
20	2	CH_3	CH_3	0.09 ± 0.06	−7.0
21	2	C_2H_5	C_2H_5	0.16 ± 0.08	−6.3
22	2	pyrrolidinyl		0.04 ± 0.03	−6.8
23	2	*N*-methylpiperazinyl		0.2 ± 0.1	−7.7
15	3	H	H	0.050 ± 0.008	−6.4
24	3	CH_3	H	0.2 ± 0.2	−6.7
25	3	C_2H_5	H	0.3 ± 0.1	−6.6
26	3	C_3H_7	H	0.17 ± 0.08	−7.5
27	3	C_4H_9	H	1.5 ± 0.5	−6.8
28	3	CH_3	CH_3	0.13 ± 0.09	−5.7
29	3	C_2H_5	C_2H_5	0.35 ± 0.09	−7.0
30	3	pyrrolidinyl		0.32 ± 0.01	−7.5
31	3	*N*-methylpiperazinyl		0.35 ± 0.06	−8.5
34	4	H	H	0.015 ± 0.004	−6.6
41	5	H	H	0.008 ± 0.002	−6.4
48	6	H	H	0.26 ± 0.01	−5.9

[a] Compounds are classified first following the length of the side chain and the substituents, then, respectively, according the mono- or disubstitution of the amino group. The IC_{50} value is the mean ± SD of 3 independent experiments.

interaction with Glu102 and/or the propionic heme group or even to reach further negatively charged residues, such as Glu116, Asp214, or the C-terminus of Ala104 (see Figure 2B). The potential binding modes of these designed compounds were analyzed by docking.

Side Chain Length Variations. The number of carbons in the alkyl side chain of 5-fluorotryptamine (compound **4**) was modified. Compound **34**, with a 4-carbon side chain length, was predicted to have the same affinity as the compounds that had 2, 3, and 5 carbon atoms (**4**, **15**, and **41**). Its predicted affinity was 1.3 kcal/mol greater than that of the 1-carbon-chain compound (compound **6**) (see Table 1). The poses found for compound **34** showed a stacking arrangement with the pyrrole ring D of the heme and the formation of two salt bridges with Glu102 and the heme propionate group (Figure 3A). Compared to 5-fluorotryptamine binding, the indole moiety penetrated deeper into the pocket on top of the heme and the fluorine atom was closer to the heme iron. There were several hydrophobic contacts with Phe99 and with the aliphatic chain of one of the heme propionates. With the 1-carbon-chain (**6**), there was less stacking and one salt bridge was lost but one additional hydrogen bond was formed between the indole NH group and the heme (Figure 3B). The fluorine atom was not oriented toward the iron atom. The compound bearing a 6-carbon side chain (**48**) featured poses in which either the stacking was lost and the side chain nitrogen made a salt bridge with Glu116 located at the entrance of the catalytic pocket or shifted stacking and the indole NH hydrogen bonds to the propionic group were maintained but no salt bridge was formed.

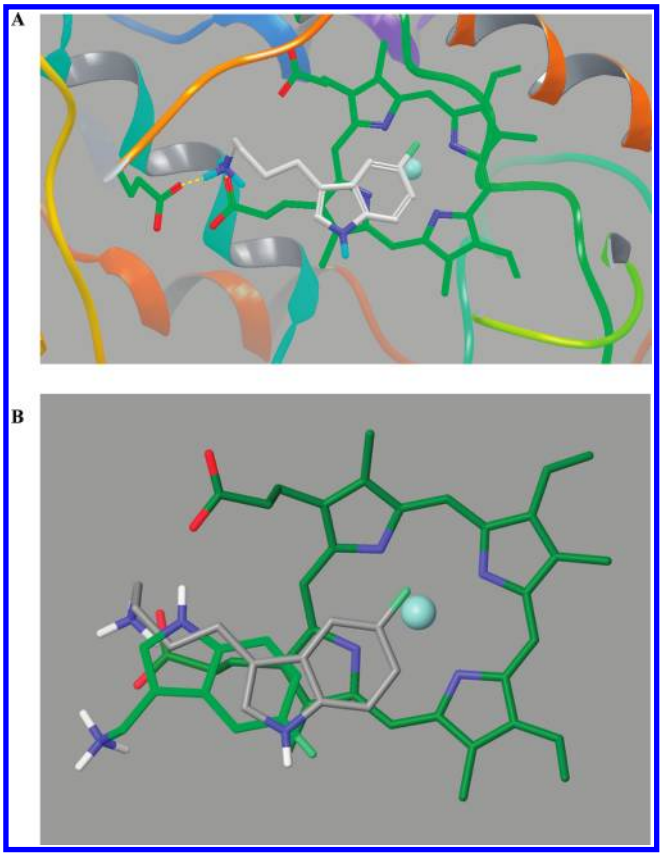

Figure 3. (A) Docking poses of compound **34** illustrating the stacking with pyrrole D of the heme and the ionic interaction with Glu102. (B) Docking poses of compound **6** and **34** illustrating the absence of ionic interaction and the poor stacking of compound **6** compared to compound **34**. The poses are generated by the Glide docking program. Compounds **6** and **34** are depicted as green and grey sticks respectively. The small blue sphere indicates the location of the ferric ion at the center of the heme.

Amino Group Side Chain Substituents. In another attempt to improve the potency of 5-fluorotryptamine, the effect of adding different substituents to the side chain amino group was analyzed. Compounds with linear or branched alkyl group substitutions on the side chain nitrogen had predicted scoring values close to those of unsubstituted compounds (see Table 1). Compound **26** had a score 1 kcal/mol more favorable than 5-fluorotryptamine (**4**). Its best pose showed hydrogen bonding to the propionic acid group and formation of a salt bridge with Glu102. Hydrophobic contacts mainly involved Phe99, Pro145, Phe146, Phe147, Phe407, Leu415, and Leu420.

We also probed cyclic groups as substituents on the amino group of the side chain in order to introduce new interactions and to reduce or avoid the energy penalty for immobilization of rotatable bonds upon binding of alkyl substituents. Two fragments were used: Pyrrolidinyl and *N*-methylpiperazinyl moieties. Compound **31** had the most favorable energy (−8.5 kcal/mol). The docked positions of this compound featured stacking with the heme pyrrole ring D, one hydrogen bond with the propionic group, an electrostatic interaction with Glu102 (not a salt bridge), and hydrophobic contacts with Phe407.

The analysis of the binding modes predicted by docking of these analogues and their binding energy values encouraged us to synthesize them for further evaluation.

Scheme 1. Synthesis of Compound **6**[a]

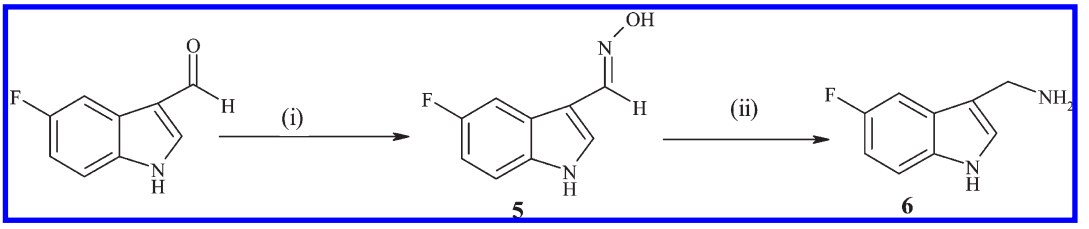

[a] Reagents and conditions (i) $NH_2OH.HCl$, pyridine; (ii) H_2, Pd/C, HCl, EtOH.

Scheme 2. Synthesis of Substituted 3-(Aminomethyl)indoles[a]

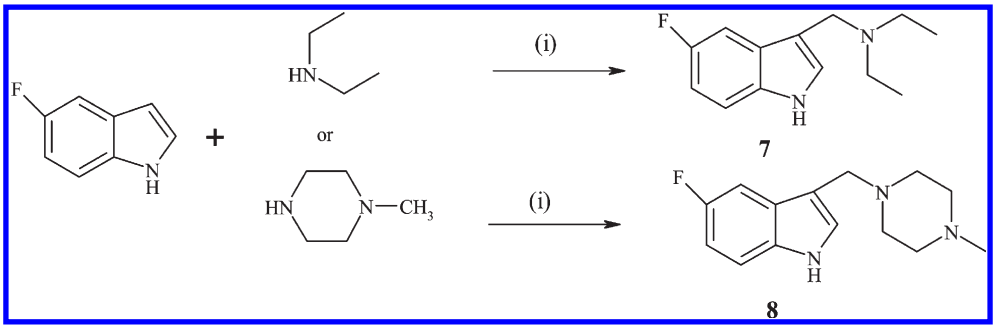

[a] Reagents and conditions: (i) formaldehyde (37 wt % aqueous solution), acetic acid, dioxane.

Scheme 3. Synthesis of the Intermediate Alcohols and Unsubstituted 3-(Aminoalkyl)indoles $n = 2$ and 3 (**4** and **15**)[a]

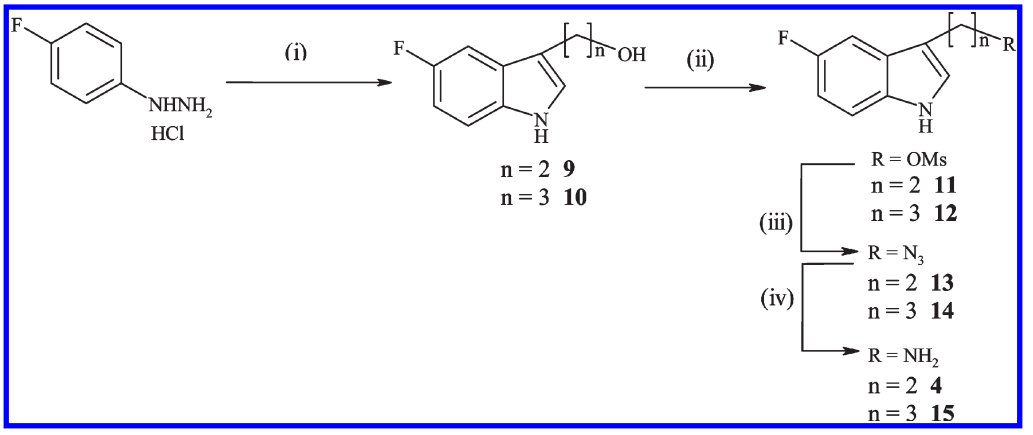

[a] Reagents and conditions: (i) dihydrofuran or dihydropyran, H_2SO_4, DMA; (ii) methanesulfonyl chloride, TEA, CH_2Cl_2; (iii) NaN_3, DMSO; (iv) H_2, Pd/C 10%, EtOH.

Chemistry. Compound **6** was prepared as indicated in Scheme 1. The carbonyl group of the commercially available 5-fluoroindole-3-carboxaldehyde was transformed into the corresponding oxime to give compound **5**.[35] Hydrogenation of the latter, catalyzed by Pd/C 10% in the presence of HCl, led to compound **6**.[36]

For the series of indoles substituted by aminomethyl moieties, aminoalkylations of commercially available 5-fluoroindole were performed using the Mannich reaction, i.e., in the presence of secondary amines and formaldehyde, resulting in the synthesis of compounds **7** and **8** (Scheme 2).[37]

For the syntheses starting from 5-fluoro-3-(hydroxyalkyl)-indoles, a general procedure based on the Fisher indole synthesis was applied using 4-fluorophenylhydrazine hydrochloride and dihydrofuran or dihydropyran for the ring formation step. To improve the results for this step, we performed the reaction described by Campos and colleagues under microwave.[38] These conditions led to shorter reaction times and higher yields (for example, 95% versus 72% for the synthesis of **9**). The starting alcohols **9** and **10** were transformed into their mesylate derivatives in good yields by adding methanesulfonyl chloride at room temperature in the presence of triethylamine. Mesylate groups were then converted into azidoalkanes to give compounds **13** and **14**, which were hydrogenated using Pd/C as catalyst to create compounds **4** and **15** (Scheme 3).[39]

To synthesize compounds **16** to **31**, which were substituted on the aliphatic nitrogen atom, mesylate derivatives **11** and **12** were added to the corresponding amines in dioxane at 100 °C (Scheme 4).[40]

To obtain 3-(4-aminobutyl)-5-fluoro-1*H*-indole oxalate **34**, the mesylate group in **12** was converted to nitrile **32**,[41] which was further hydrolyzed by KOH in *t*-BuOH to give carboxamide **33**.[42] Reduction of the amide using $LiAlH_4$ in dioxane led to the desired amine **34** (Scheme 5).[43]

The synthesis of compound **41** followed the same synthetic path as for the indole derivative **34** but started from

Scheme 4. Synthesis of Compounds **16**−**31**[a]

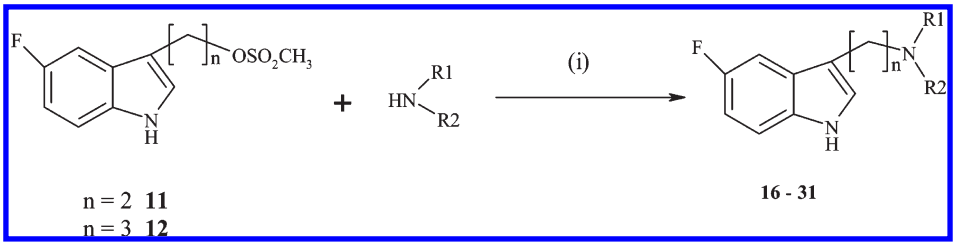

[a] Reagents and conditions: (i) dioxane, 100 °C.

Scheme 5. Synthesis of Compound **34**[a]

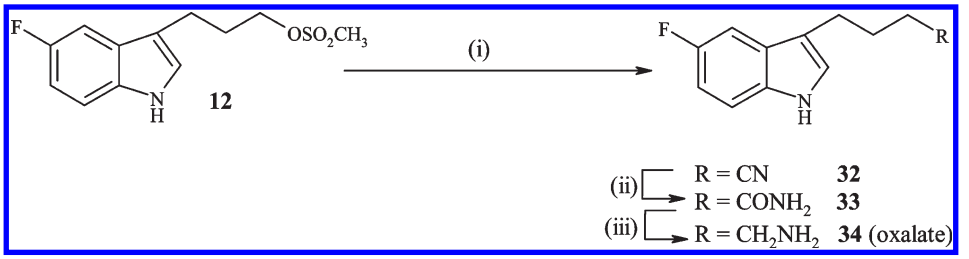

[a] Reagents and conditions: (i) NaCN, H_2O, DMA, 100 °C; (ii) KOH, *t*-BuOH; (iii) $LiAlH_4$, dioxane, 100 °C.

Scheme 6. Synthesis of Compound **41**[a]

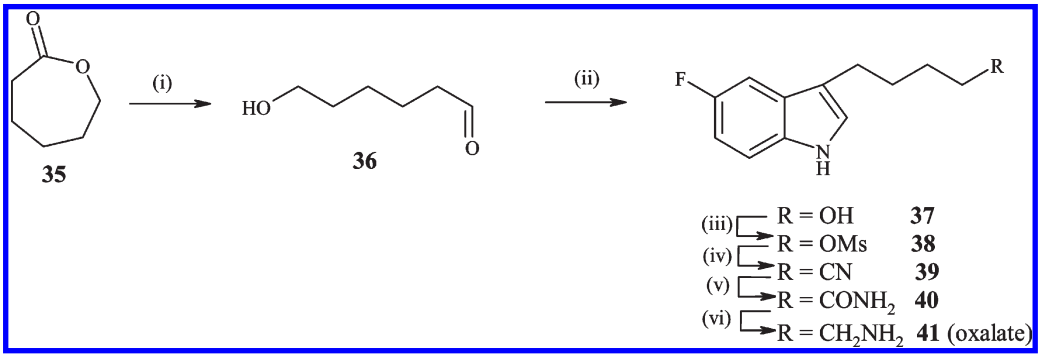

[a] Reagents and conditions: (i) DIBAL-H, CH_2Cl_2, −78 °C; (ii) 4-fluorophenylhydrazine hydrochloride, H_2SO_4, DMA; (iii) methanesulfonyl chloride, TEA, CH_2Cl_2; (iv) NaCN, H_2O, DMA, 100 °C; (v) KOH, *t*-BuOH; (vi) $LiAlH_4$, dioxane, 100 °C.

6-hydroxyhexanal **36**, which was obtained by the reduction of ε-caprolactone **35** using DIBAL-H (Scheme 6).[44] The aldehyde was then subjected to a Fisher reaction with 4-fluorophenylhydrazine hydrochloride, giving the alcohol **37**, which was further converted into the mesylate **38**. A nucleophilic substitution was performed on compound **38** using NaCN, and the resulting nitrile **39** was then hydrolyzed into the amide **40**. After reduction of the latter by $LiAlH_4$, the final compound (**41**) was isolated as its oxalate salt.

Finally, the fluorotryptamine derivative with 6 methylene groups in the side chain was obtained, starting from cyclooctanone **42** after a Baeyer−Villiger rearrangement and reduction of the resulting lactone **43** into aldehyde **44** (Scheme 7).[45] The usual synthetic scheme was then used, as for compound **4** synthesis.

Biological Activity. A microplate reader was used to monitor inhibition of MPO-mediated taurine chlorination in a high throughput screening mode.[46] Table 1 lists the IC_{50} values of the 3-(aminoalkyl)-5-fluoroindole analogues. The presented IC_{50} values clearly demonstrate that the capacity of the investigated compounds to inhibit MPO-mediated chlorination was modulated by the length of the aminoalkyl side chain on position 3 of 5-fluoroindole, as well as by the alkyl groups substituting its amino group. Compound **41** with a 5-carbon nonsubstituted side chain was the most efficient inhibitor. Lengthening the side chain from $n = 1$ to $n = 5$ increased the inhibitory potency. With the exception of substitution by dimethyl or pyrrolidinyl groups, substitution of the side chain nitrogen did not improve the inhibition. Compound **27** with a 3-carbon chain and a butyl substituent displayed the weakest activity. A closer analysis of compounds that had the same side chain length but different substituents revealed striking features. Among the molecules with a 2-carbon side chain, compound **22** with a pyrrolidine and compound **20** with a dimethylamino group exhibited the greatest activity. In this series, the size of the alkyl substituents (except for very bulky groups) apparently did not affect the inhibitory potency (compound **19**). In the 3-carbon side chain series, the unsubstituted indole **15** had the most inhibitory activity. In this series, the volume of the substituents did not significantly change the interaction with MPO (as for 2-carbon side chain molecules). Finally, among all the fluorotryptamine derivatives, the 1-carbon chain compounds displayed marginal inhibitory activities.

Scheme 7. Synthesis of Compound **48**[a]

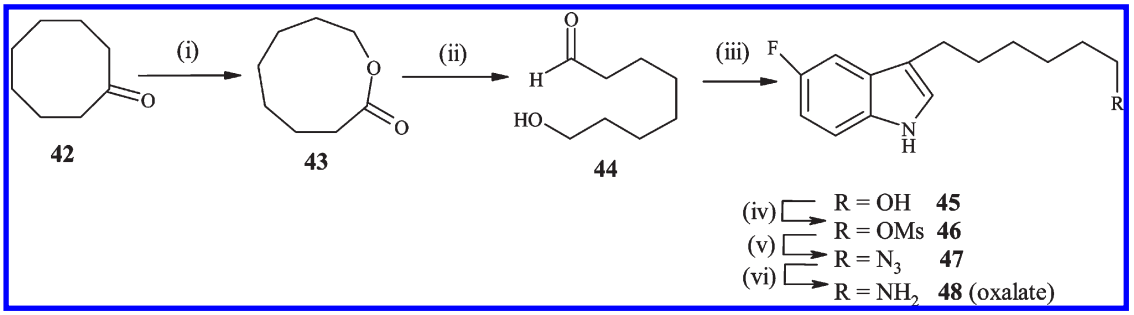

[a] Reagents and conditions: (i) *m*-chloroperbenzoic acid, CH_2Cl_2, 70 °C; (ii) DIBAL-H, CH_2Cl_2, −78 °C; (iii) 4-fluorophenylhydrazine hydrochloride, H_2SO_4 4%, DMA; (iv) methanesulfonyl chloride, TEA, CH_2Cl_2; (v) NaN_3, DMSO, 100 °C; (vi) H_2, Pd/C 10%, EtOH.

Table 2. IC_{50} Values for the Inhibition of the Oxidation of LDL Carried Out by MPO/Cl^-/H_2O_2

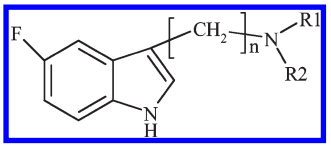

no.	*n*	R_1	R_2	IC_{50} (μM)
6	1	H	H	> 1[a]
7	1	C_2H_5	C_2H_5	> 1[a]
8	1	N-methylpiperazinyl		> 1[a]
4	2	H	H	0.94[a]
16	2	CH_3	H	0.65[a]
17	2	C_2H_5	H	0.85[a]
18	2	C_3H_7	H	0.46[a]
19	2	C_4H_9	H	0.25[a]
20	2	CH_3	CH_3	0.58[a]
21	2	C_2H_5	C_2H_5	0.51[a]
22	2	pyrrolidinyl		1.03[a]
23	2	*N*-methylpiperazinyl		0.65[a]
15	3	H	H	0.65[a]
24	3	CH_3	H	0.026[b]
25	3	C_2H_5	H	0.19[a]
26	3	C_3H_7	H	0.34[a]
27	3	C_4H_9	H	0.017[b]
28	3	CH_3	CH_3	0.049[b]
29	3	C_2H_5	C_2H_5	0.39[a]
30	3	pyrrolidinyl		0.21[b]
31	3	*N*-methylpiperazinyl		0.31[a]
34	4	H	H	0.012[b]
41	5	H	H	0.005[b]
48	6	H	H	0.58[a]

[a] IC_{50} values calculated by measuring the inhibition of the LDL oxidation at three concentrations (1000, 100, and 50 nM; see Supporting Information). [b] IC_{50} values were calculated from sigmoid curves obtained by measuring the inhibition with seven concentrations (5.0, 7.5, 10.0, 25.0, 50.0, 500.0, 1000.0 nM).

To measure MPO-dependent LDL oxidation, which is a contributing factor in atherogenesis, an ELISA was recently developed, based on a mouse monoclonal antibody (Mab AG9) that specifically recognizes MPO-oxidized APO B-100 on LDL.[30] Table 2 lists the IC_{50} values for the inhibition of LDL oxidation by the different compounds. Most of the compounds described in this study effectively inhibited LDL oxidation at submicromolar concentrations. Compounds **34** and **41** and, to a lesser extent, **24** and **27**, showed the best inhibition profile. Other compounds with a 3-carbon side chain also exhibited rather good inhibitory activity (except compound **15**). For comparison, indoles with a 2-carbon side chain had less inhibitory potency and compounds with a 1-carbon side chain were weak inhibitors of LDL oxidation.

Two compounds, however, attracted attention. Compound **27** had a poor inhibitory effect on MPO-mediated taurine chlorination but was an excellent inhibitor of LDL oxidation. In contrast, compound **22** had a small effect on LDL oxidation (except at the higher concentration) despite a marked effect on the chlorination activity of MPO.

Two redox intermediates are relevant in the enzymology of MPO, namely Compound I and Compound II. Because tryptamine derivatives have been shown to act as reversible inhibitors and interact with both redox intermediates,[31] it was important to also study the direct interaction of the most efficient inhibitors (compounds **34** and **41**) with Compound I and Compound II by sequential-mixing stopped-flow spectroscopy (Figures 5 and 6).[47] Compound I is formed by the reaction of hydrogen peroxide with the ferric state of MPO (Figure 4). Thereby, the O−O bond is cleaved heterolytically, forming a redox intermediate called Compound I. In this fast reaction, Fe(III) is oxidized to an oxoferryl species [Fe(IV)═O] and the porphyrin to the corresponding π−cation radical (reaction 1 in Figure 4). Compound I is deficient in two electrons and restoration of the ferric state can be accomplished by either direct two-electron reduction by halides (Cl^- or Br^-), thereby forming the corresponding hypohalous acids (reaction 2 in Figure 4), or by two one-electron reduction steps mediated by aromatic electron donors (including indole derivatives) via Compound II [Fe(IV)-OH] (reactions 3 and 4 in Figure 4).[49] The halogenation cycle includes reactions 1 and 2, whereas the peroxidase cycle includes reactions 1, 3, and 4. It is important to note that Compound II cannot oxidize chloride or bromide.

Figures 5 and 6 demonstrate the kinetics of the reactions between compound **34** and MPO Compound I and Compound II. Very similar time traces were observed with compound **41** (not shown). The inhibitors acted as one-electron donors to both redox intermediates of MPO. Figure 5 depicts the direct transition of Compound I to Compound II mediated by oxidation of compound **34**. The reaction was monophasic (Figure 5B), and from the linear dependence of k_{obs} values on substrate concentration, apparent bimolecular rates (k_3) of $(1.1 \pm 0.1) \times 10^7$ M^{-1} s^{-1} (compound **34**) and $(1.0 \pm 0.1) \times 10^7$ M^{-1} s^{-1} (compound **41**) were calculated (Figure 5C). The high intercept clearly demonstrated that Compound II was not stable but further transformed. This is highlighted by Figures 6A and 6B that show the direct monophasic transition of Compound II to native MPO mediated by compound **34** with a clear isosbestic point. The apparent bimolecular rate constants (k_4) were

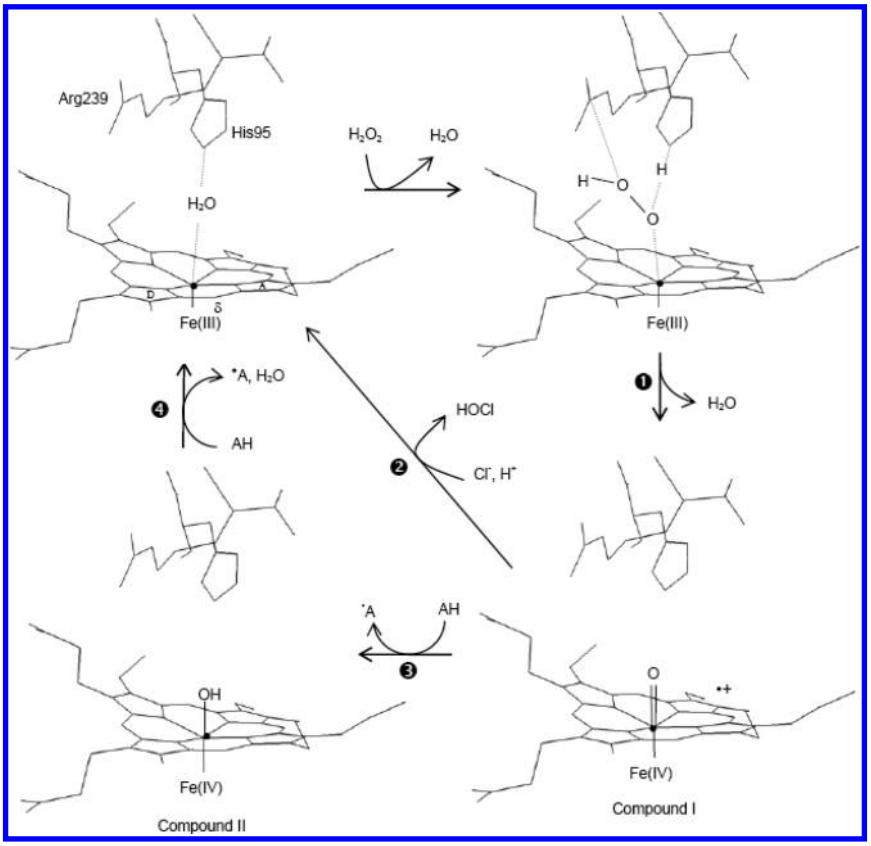

Figure 4. Scheme of chlorination cycle and peroxidase cycle of myeloperoxidase (MPO). Architecture of heme and conserved distal residues His95 and Arg239 was obtained from X-ray structure (PDB: 1CXP). At the heme edge (δ-meso bridge between pyrrol rings A and D), substrates bind and donate electrons. In reaction (1): ferric MPO is oxidized by hydrogen peroxide to Compound I [i.e., oxoiron(IV) porphyrin radical cation]. In reaction (2), Compound I is directly reduced back to the resting state by chloride (or bromide) thereby releasing hypochlorous (or hypobromous) acid. Reactions (1) and (2) constitute the halogenation cycle. In reaction (3), Compound I is reduced to Compound II [i.e., protonated oxoiron(IV)] by a one-electron donor (e.g., an indole derivative). In reaction (4), Compound II is reduced to the native state thereby oxidizing a second substrate molecule. Reactions (1), (3), and (4) constitute the peroxidase cycle. Note that Compound II cannot oxidize chloride or bromide.

360 M^{-1} s^{-1} (compound **34**) and 506 M^{-1} s^{-1} (compound **41**) (Figure 6C). The k_3/k_4 ratios of 30555 and 19762 suggest that Compound II reduction was the rate limiting step in the peroxidase cycle. Both inhibitors were excellent electron donors for Compound I, but poor substrates for Compound II.

Discussion and Conclusions

We used structure-based docking of 5-fluorotryptamine (**4**) in the active site of MPO to design derivatives with potent inhibitory action against MPO (see Table 1 and 2). All the designed derivatives could be docked into the active site pocket. The best poses featured stacking between the indole and the pyrrole moieties although this interaction was not ideal in all cases. The docking energy binding values of these compounds ranged between −5.3 and −8.5 kcal/mol with a value of −6.5 kcal/mol for 5-fluorotryptamine (**4**). Given the difficulty in evaluating affinity using the scoring functions developed for the docking programs, we could not reliably discriminate between the different ligands, and as a result, all the designed compounds were synthesized and their IC_{50} values were measured.

In unsubstituted compounds, the distance between the indole moiety and the side chain nitrogen atom appeared to be an important parameter for binding to, and inhibition of, MPO. Lengthening the side chain from 1 to 5 carbons increased the inhibitory potency by 2 orders of magnitude. The docked poses provide a tentative explanation for the high IC_{50} value for the 1-carbon side chain; because of the short alkyl chain, the nitrogen group cannot reach the negatively charged Glu102 to form a salt bridge, as observed for the 2-, 3-, 4-, and 5-carbon side chains. However, a further increase to a 6-carbon side chain again increased the IC_{50}.

In contrast, in 2- and 3-carbon side chain compounds, the inhibitory potency decreased when the side chain amino group was substituted with linear alkyl substituents of increasing length. In most cases, compounds with an N-substituted side chain showed higher IC_{50} values compared to unsubstituted compounds with the same side chain length. However, compounds with two substituents had more favorable inhibitory properties compared to those with just one linear substituent (e.g., compare compound **19** with compound **21** or compound **27** with compound **29**). The docked poses suggest that disubstituted amino groups fit better into the hydrophobic pocket of MPO.

Compounds with cyclic substituents were not potent inhibitors, with the exception of compound **22**. The experimental data and the docked binding modes suggest that the steric hindrance on the side chain amino group and the flexibility of the substituents may be important factors for the structure−activity relationship.

There was no clear correlation between the calculated docking binding energies and the IC_{50} values derived from the two in vitro inhibition assays. This illustrates that molecular docking

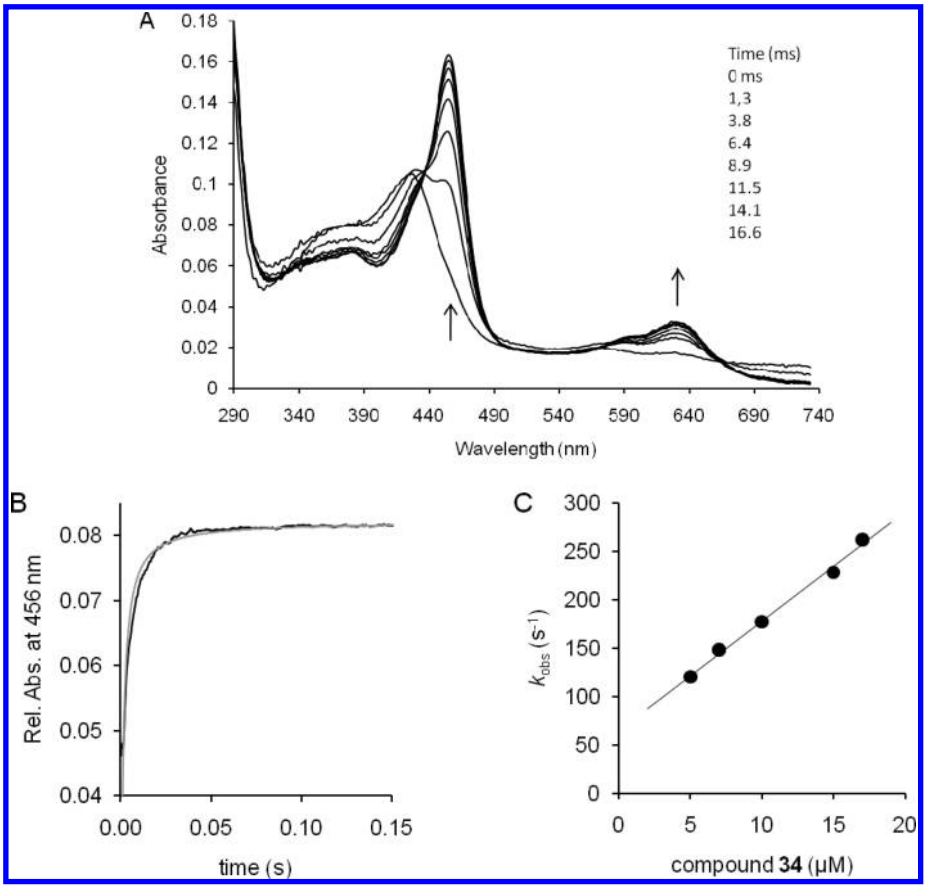

Figure 5. Reaction of MPO Compound I with compound **34** (pH 7.4 and 25 °C). (A) Spectral changes upon reaction of 2 μM MPO Compound I with 10 μM compound **34**. First spectrum after mixing corresponds to Compound I subsequent spectra were recorded after 1.3, 3.8, 6.4, 8.9, 11.5, 14.1, and 16.6 ms. Arrows indicate spectral changes. (B) Typical time trace and fit of MPO Compound II formation followed at 456 nm. (C) Pseudo-first-order rate constants for MPO Compound I reduction plotted against compound **34** concentration.

may be helpful in predicting binding modes of a molecule to an active site but cannot easily be used for ranking the inhibitory capacity. In the present study, the inhibiting molecules were also substrates and their efficiency to interact with MPO Compounds I and II depended also on the redox potential of the bound molecule itself, which is not necessarily correlated with the binding affinity. As a result of the poor scoring correlation, "induced-fit" studies were undertaken for two compounds selected as the least and most potent inhibitors (**27** and **34**). Docked poses differed only by the positions of their side chains and the scored affinity shifted from −6.8 to −5.8 and from −6.6 to −7.6 kcal/mol for compounds **27** and **34**, respectively. This observation suggests that "induced-fit" effects could be important for binding of fluorotryptamine analogues.

Inhibition parameters for LDL oxidation are relevant because they reflect the potential in vivo effects of the compounds (see Table 2). One of the most striking observations is that substitution by *N*-methylpiperazinyl in the compounds with 2-carbon side chains increased the inhibitory potency in comparison with structurally closely related compounds in terms of chain length and steric hindrance (for example, compare compounds **22** and **23**). Compound **23** was the weakest in its series in the MPO chlorination inhibition assay (see Table 1) but had a very good activity in the inhibition of LDL oxidation (see Table 2). The reason for this sudden increase in LDL oxidation inhibitory activity for compound **23** is unknown and might be ascribed to the presence of a second nitrogen. The second important observation is the very marked activity of compounds **34** and **41**, which was corroborated by the inhibition of taurine chlorination. A relationship between inhibition of taurine chlorination and of LDL-oxidation is obvious for the most potent inhibitors. This demonstrates that these different molecules were able to inhibit LDL oxidation in spite of the binding between MPO and LDL.[48] Binding of MPO to LDL during LDL oxidation is responsible for the oxidative modification of APO B-100 in plasma. However, this event could also block the catalytic site of the enzyme and, therefore, interfere with enzymatic inhibition by providing some protective effect.[16] The heme group of MPO that is responsible for the enzymatic activity is indeed located in a distal hydrophobic cavity with a narrow oval-shaped opening.[30] This characteristic might explain the observed differences in the inhibition of MPO-mediated taurine chlorination and LDL oxidation. As far as binding to LDL is concerned, the lipophilicity of potent inhibitors seems to be an important factor. Indeed, the formation of a complex macromolecular structure between MPO and LDL, mainly through electrostatic interactions, may modify the chemical and steric requirements for good penetration of substrates and/or inhibitors into the heme cavity. Parameters such as charge and lipophilicity of compounds have already been evoked to explain similar results.[16,30]

The transient kinetics study demonstrated that the probed compounds act as electron donors of both relevant redox intermediates of MPO, namely Compound I and Compound II. Detailed kinetic parameters could be elucidated for the most potent inhibitors, compounds **34** and **41**. Substrates for MPO (halides or aromatic compounds) have been demonstrated to

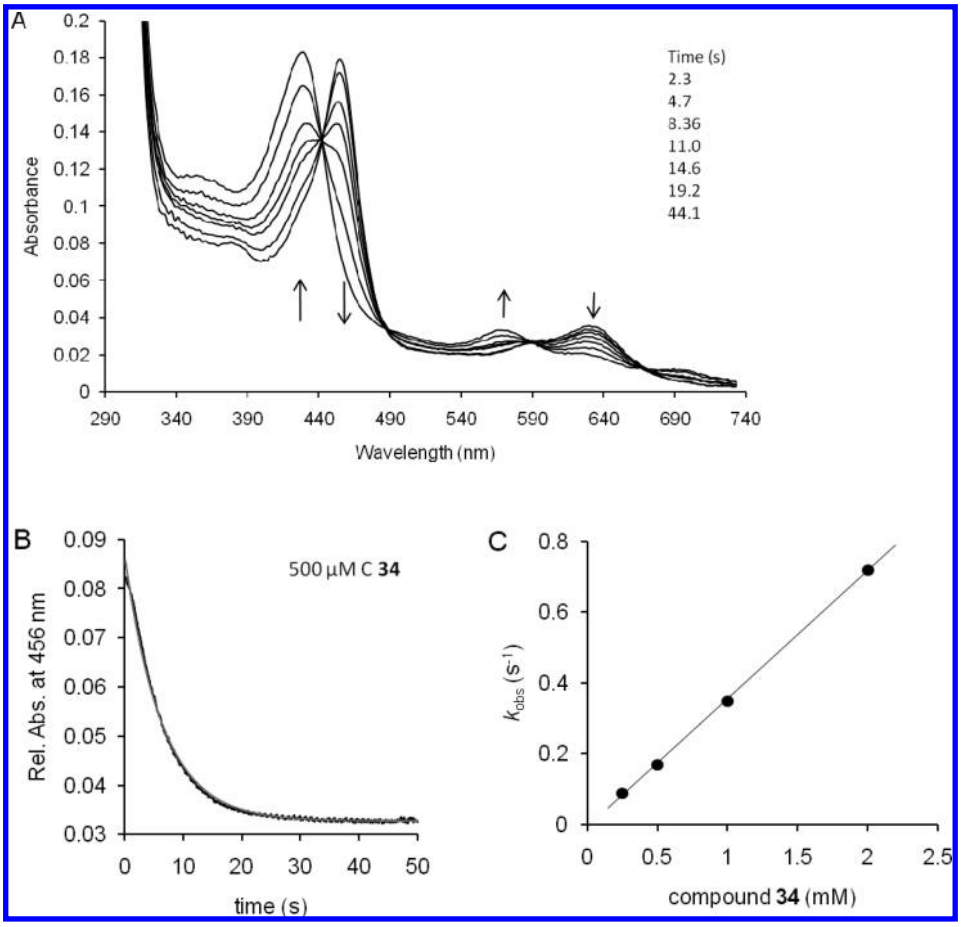

Figure 6. Reaction of MPO Compound II with compound **34** (pH 7.4 and 25 °C). (A) Spectral changes upon reaction of 2 μM MPO Compound I with 500 μM compound **34**. First spectrum after mixing corresponds to Compound II, subsequent spectra were recorded after 2.3, 4.7, 8.36, 11, 14.6, 19.2, and 44.1 s. Arrows indicate spectral changes. (B) Typical time trace and fit of MPO Compound II reduction followed at 456 nm. (C) Pseudo-first-order rate constants for MPO Compound II reduction plotted against compound **34** concentration.

bind and deliver electrons at the entrance to the distal heme pocket near the δ-meso bridge (between pyrrol ring A and D; see Figure 4),[49,50] which is supported by the presented docking data. It is reasonable to assume that substrate binding sites at Compounds I and II are identical. This assumption is based on the fact that structural differences in the heme pocket even between (high-spin) ferric MPO and its (low-spin) cyanide complex are negligible.[50] The cyanide complex of a peroxidase is a suitable model for the (low-spin) oxoferryl-state of Compound I and Compound II.[50] Consequently, the observed differences between the apparent reaction rates, k_3 and k_4, must be the result of differences in the redox properties of Compound I and Compound II. Because of the very high reduction potential of MPO Compound I, both inhibitors were rapidly oxidized, thereby directly reducing Compound I to Compound II.[49] Compared to Compound I, Compound II is a weaker oxidant, as reflected by high k_3/k_4 ratios. Similar findings have been reported for 5-fluorotryptamine, suggesting that these compounds act as reversible inhibitors.[31] Because of their marked efficiency in one-electron reduction of Compound I, they shift MPO from the chlorination cycle to the peroxidase cycle (Figure 4) because Compound II is not able to oxidize chloride or bromide. The MPO-typical high difference in reduction potentials between Compounds I and II (which is not observed in homologous lactoperoxidase or eosinophil peroxidase) guarantees that a high percentage of MPO stays as Compound II and that other human heme peroxidases cannot oxidize these inhibitors. As a result, the new tryptamine analogues decrease the pool of native MPO and Compound I responsible for the oxidative damage and do not interfere with homologous peroxidases.

In conclusion, a series of 3-(aminoalkyl)-5-fluoroindole analogues was designed using structure-based docking of 5-fluorotryptamine. These compounds were synthesized and assessed in vitro. Some of these compounds showed considerable potency for inhibition of taurine chlorination and of LDL oxidation mediated by MPO. The more potent molecules possess a 4- or 5-carbon length side chain and no substituent on the side chain nitrogen. These are the first molecules that have been shown to inhibit LDL oxidation in vitro at nanomolar concentrations, thus providing an excellent basis for further development of drugs targeting MPO. The discrepancies observed in the different MPO inhibition assays (Table 1 and Table 2) provide insight into the interaction between MPO and LDLs during LDL oxidation, which can be further studied in in vivo experiments.

Experimental Section

Docking Experiments. Protein and Ligand Preparation. The X-ray structure of human myeloperoxidase complexed to cyanide and thiocyanate (PDB code: 1DNW) was used as the target structure to endeavor the docking studies.[50] The X-ray water and CN^- and SCN^- molecules were removed from the active site. The ligand input files were prepared according to the following procedure. The initial 3D structures of the ligands

were generated using Corina,[51] and the ligand partial charges were ascribed using the OPLS force-field as performed by Glide.[52] As part of an effective 3D ligand structure preparation process the Epik program was used to predict pK_a values and generate protonation states of all ligands.[53] All ligands feature pK_a values higher than 8.5 for their side chain nitrogen. They were thus docked in their protonated form.

Docking Procedure. The Glide (Grid-Based Ligand Docking With Energetics) algorithm approximates a systematic search of positions, orientations, and conformations of the ligand in the receptor binding site using a series of hierarchical filters (www.schrödinger.com). In the present work, the binding region was defined by a 18 Å × 18 Å × 18 Å box centered on the central position of the cyanide in the crystal complex. At most 10 poses were generated for each molecule. The protein structure was prepared using the Protein Preparation Wizard in the Schrödinger software graphical user interface Maestro. Glide XP docking protocol and scoring function were used to score the poses of the different ligands. The default settings of Glide version 4.5 were used for the remaining parameters. Induced-fit protocols were performed for compound **34** and **27**. Initial Glide docked poses were obtained in binding sites with Phe99, Glu102, Arg239, and Phe407 mutated into alanine. Side-chain and backbone minimizations as well as docked poses refinement were carried out in structures with the alanine side chains replaced by their wild type corresponding residues. Glide redockings were carried out in these minimized structures.

Synthesis. ^1H and ^{13}C NMR spectra were taken on a Bruker Avance 300 spectrometer at 293 K (Bruker, Wissembourg, France). δ are given in ppm relative to TMS, and the coupling constants are expressed in Hz (frequencies for ^1H and ^{13}C: respectively 300 and 75 MHz). IR analyses were performed on a Shimadzu IR-470 spectrophotometer and the peaks data are given in cm^{-1}. The mass spectra were obtained on QTOF 6520 (Agilent, Palo Alto, CA, USA), positive mode, ESI, mode TOF, by diffusion of 0.5 mL/min, with mobile phase HCOOH 1%: CH_3OH (50:50), (VCAP 3500 eV; Source T°, 350 °C; fragmentor, 110 V; Skinmer, 65 V). All reactions were followed by TLC carried out on Fluka PET-foils Silica Gel 60 and compounds were visualized by UV and by spraying Van Urk reagent (0.13 g of *p*-dimethylaminobenzaldehyde dissolved in a mixture of 100 mL of 65 wt % H_2SO_4 and 0.1 mL of 5 wt % $FeCl_3$). Column chromatographies were performed with EchoChrom MP silica 63-200 from MP Biomedicals. The starting compounds 4-phenylhydrazine hydrochloride, dihydrofuran, dihydropyran, and 5-fluoroindole were available from Sigma-Aldrich. Starting compound 5-fluoroindole-3-carboxaldehyde was purchased from Alfa Aesar. Reactions under microwave were performed with a Start-S microwave oven from Milestone (Milestone, Sorisole, Italy). Purity was determined with LC-DAD (Waters, Milfors, USA) using a 150 mm × 4.6 mm Symmetry C_{18} column at a mobile phase flow rate of 1 mL/min. The mobile phase was a mixture of methanol (350 mL) and a KH_2PO_4 solution (0.07 M in water, 650 mL) adjusted to pH 3.0 with a 34 wt % H_3PO_4 solution. The chromatograms were extracted at maximum absorption wavelengths by using the Max Plot extraction mode. The purity was ≥95% for all the compounds.

General Procedures. General Procedures for the Synthesis of Compounds 4, 15, and 48. Palladium on charcoal 10% (50 mg) was added to a solution of azide derivative (4.6 mmol) in EtOH (20 mL). The suspension was stirred under H_2 (4.1 bar) overnight. After filtration on Celite, the solvent was evaporated under reduced pressure. The residue was dissolved in ether, extracted with 0.1 M HCl, and the resulting solution was washed with ether. A solution of 1 M NaOH was added (pH ≈ 10), and the mixture was extracted with diethylether. The organic layer was washed with water, dried over Na_2SO_4, and evaporated under reduced pressure. For compound **4**, a saturated solution of anhydrous oxalic acid in ether was added to the ethereal solution and the resulting solid was filtered, washed with ether, and dried under vacuum.

General Procedures for the Synthesis of Compounds 7 and 8. To a solution of 5-fluoroindole (200 mg, 1.6 mmol) in dioxane (5 mL) was added a mixture of the amine (1.6 mmol) and formaldehyde (145 μL, 37 wt % solution in water) in dioxane/acetic acid 1:1 (6 mL). The resulting mixture was stirred at room temperature overnight and the solvent was evaporated under reduced pressure. To the residue, a solution of 0.1 M KOH (30 mL) and EtOAc were added. Then the organic layer was washed with water, dried with Na_2SO_4, and evaporated under vacuo. The residue was dissolved in diethylether and extracted with 0.1 M HCl. The aqueous layer was rendered alkaline with 1 M KOH (pH ≈ 10) and extracted with diethylether. The organic layer was dried on Na_2SO_4 and evaporated

General Procedure for the Synthesis of Compounds 9, 10, 37, and 45.[38] A solution of 4-fluorophenylhydrazine hydrochloride (1 g, 6.9 mmol) in 4 wt % aqueous H_2SO_4 (10 mL) and DMA (10 mL) was heated at 100 °C under microwave. To this solution was added dihydrofuran, dihydropyran, or the corresponding hydroxyaldehyde (6.9 mmol) dropwise over 2 min. Then the reaction was heated at 175 °C (temperature ramp from room temperature to 100 °C over 8 min, then addition of the reagent, heating to 175 °C over 8 min and maintaining this temperature for 30 min, 1000 W). The reaction mixture was cooled to room temperature and extracted two times with EtOAc (25 mL), and the organic layer was washed with water and evaporated. The crude material was purified by column chromatography (eluent CH_2Cl_2/EtOAc 4:1).

General Procedure for the Synthesis of Compounds 11, 12, 38, and 46.[54] A solution of alcohol (5.5 mmol) in CH_2Cl_2 (25 mL) was cooled with an ice bath. To this solution TEA (0.44 mL, 5.8 mmol) and methanesulfonyl chloride (0.77 mL, 5.5 mmol) were added. The solution was stirred at room temperature for 2 h. Then it was washed with a saturated solution of $NaHCO_3$ and H_2O and then dried over Na_2SO_4 and filtered. The solvent was evaporated under reduced pressure. The crude material was purified by flash chromatography (CH_2Cl_2/EtOAc 4:1).

General Procedure for the Synthesis of Compounds 13, 14, and 47.[55] To a solution of sulfonate (3.6 mmol) in DMSO (20 mL), NaN_3 (3.6 mmol) was added, and the solution was stirred at room temperature for 4 h (compounds **13** and **14**) or for 1 h at 100 °C (compound **47**) . Then H_2O (30 mL) and toluene (30 mL) were added. After decantation, the organic layer was washed with water, dried with Na_2SO_4, filtered, and evaporated under reduced pressure. The residue was purified by column chromatography (CH_2Cl_2).

General Procedure for the Synthesis of Compounds 16−31. A solution of mesylate **11** or **12** (3.6 mmol) in dioxane (5 mL) was added slowly through an addition funnel to a refluxing solution of the amine (0.26 mol) in dioxane (15 mL) at 100 °C. After the addition was completed, the reaction medium was stirred at this temperature for 4 h. After cooling, the mixture was treated with water (20 mL) and extracted with EtOAc (30 mL). The organic layer was dried over Na_2SO_4 and evaporated to dryness to afford a crude product. The residue was dissolved in 0.1 M HCl. This solution was washed with diethylether and rendered alkaline (pH ≈ 10) with a solution of 1 M NaOH. The mixture was extracted with ether. The organic layer was washed with water, dried over Na_2SO_4, and evaporated to afford the crude base as a solid. When bases were obtained as liquids, corresponding tartaric acid salts were prepared according to the following method. After evaporation of ether, the residue was taken up with a hot solution of D-tartaric acid (1 equivalent) in 2-propanol (10 mL). The mixture was cooled and the formed solid was filtered and dried under vacuum.

General Procedure for the Synthesis of Compounds 32 and 39. To a solution of NaCN (2 g, 41 mmol) in H_2O (10 mL), DMA (10 mL) was added and heated at 100 °C. Then, a solution of the mesylate (7.4 mmol) in DMA (10 mL) was added dropwise. The reaction was stirred at this temperature for 2 h and then cooled to room temperature and extracted with EtOAc. The organic layer

was washed with water, dried on Na_2SO_4, and evaporated. The residue was purified by flash chromatography (CH_2Cl_2/EtOAc 4:1).

General Procedure for the Synthesis of Compounds 33 and 40. To a solution of nitrile (11 mmol) in *t*-BuOH (40 mL) was added finely powdered KOH (5 g, 89 mmol). The solvent was refluxed for 2 h with stirring. Then a saturated solution of NaCl (50 mL) was added and the resulting mixture was extracted three times with CH_2Cl_2. Flash chromatography was performed (CH_2Cl_2/EtOAc 4:1 then CH_2Cl_2/methanol 1:1). The fractions obtained with the second solvent mixture were evaporated.

General Procedure for the Synthesis of Compounds 34 and 41. The amide compound (7.7 mmol) was dissolved in dioxane (50 mL) and $LiAlH_4$ (1.0 M solution in dioxane, 25 mL) was added. The suspension was refluxed for 3 h, the reaction was quenched with ice and a 15 wt % KOH aqueous solution (10 mL). The mixture was filtered through Celite and extracted with EtOAc (30 mL). The organic layer was extracted with 0.1 M HCl and, after decantation, the aqueous phase was washed with diethylether. A 1 M KOH solution was added to the acidic layer (pH $\approx$ 10) and this was extracted with diethylether. The solvent was dried on Na_2SO_4 and evaporated. The residue was dissolved in diethylether, and a saturated solution of anhydrous oxalic acid in diethylether was added dropwise. The precipitate was filtered, washed with ether, and dried at 40 °C under reduced pressure.

General Procedure for the Synthesis of Compounds 36 and 44. A 1 M DIBAL-H solution in CH_2Cl_2 (7.8 mL, 7.38 mmol) was added slowly to a solution of the lactone (6.6 mmol) in dry CH_2Cl_2 at −78 °C. After stirring at the same temperature for 1 h, methanol (8.9 mL) was added dropwise and the mixture poured into 0.5 M HCl (200 mL). After stirring for additional 1 h at room temperature, the organic layer was separated. The aqueous layer was extracted with CH_2Cl_2 (3 × 20 mL), and the combined organic layers were dried with Na_2SO_4 and evaporated. The residue purified by flash chromatography (first CH_2Cl_2, then CH_2Cl_2:EtOAc (60:40)). The second fraction was evaporated to give the desired product.

Pharmacological Tests. Myeloperoxidase Inhibition Assay. The assay was based on the production of taurine chloramine produced by the MPO/H_2O_2/Cl^- system in the presence of a selected inhibitor at defined concentration.[46] The reaction mixture contained the following reagents in a final volume of 200 μL: pH 7.4 phosphate buffer (10 mM PO_4^{3-}/300 mM NaCl), taurine (15 mM), the compound to be tested (up to 20 μM), and the fixed amount of the recombinant MPO (6.6 μL of MPO batch solution diluted 2.5 times, 40 nM). When necessary, the volume was adjusted with water. This mixture was incubated at 37 °C and the reaction initiated with 10.0 μL of H_2O_2 (100 μM). After 5 min, the reaction was stopped by the addition of 10 μL of catalase (8 U/μL). To determine the amount of taurine chloramines produced, 50 μL of 1.35 mM solution of thionitrobenzoic acid were added and the volume adjusted to 300 μL with water. Then, the absorbance of the solutions was measured at 412 nm with a microplate reader and the curve of the absorbance as a function of the inhibitor concentration was plotted. IC_{50} values were then determined using standard procedures taking into account the absence of hydrogen peroxide as 100% of inhibition and the absence of inhibitors as 0% of inhibition.[16]

Determination of LDL Oxidation Inhibition. Preparation of the Recombinant Enzyme and of LDL. Recombinant MPO was prepared as previously described. Each batch solution is characterized by its protein concentration (mg/mL), its activity (U/mL), and its specific activity (U/mg). The chlorination activity was determined according to Hewson and Hager.[56] Human plasma served for the isolation of LDL by ultracentrifugation according to Havel et al.[57] Before oxidation, the LDL fraction ($1.019 < d < 1.067$ g/mL) was desalted by two consecutive passages through PD10 gel-filtration columns (Amersham Biosciences, The Netherlands) using PBS buffer. The different steps were carried out in the dark, and the protein concentration was measured by the Lowry assay for both MPO and LDL.

Inhibition of LDL Oxidation. LDL oxidation was carried out at 37 °C in a final volume of 500 μL. The reaction mixture contained the following reagents at the final concentrations indicated between brackets: pH 7.2, PBS buffer, MPO (1 μg/mL), LDL (1000 μg/mL), 2 μL 1 N HCl (4 mM), one of the drugs at different concentrations, and H_2O_2 (100 μM). The reaction was stopped after 5 min by cooling the tubes in ice. The assay was performed as described by Moguilevsky et al. in a NUNC maxisorp plate (VWR, Zaventem, Belgium): 200 ng/well of LDL was coated overnight at 4 °C in a sodium bicarbonate pH 9.8 buffer (100 μL).[58] Afterward, the plate was washed with TBS 80 buffer and then saturated during 1 h at 37 °C with the PBS buffer containing 1% BSA (150 μL/well). After washing the wells twice with the TBS 80 buffer, the monoclonal antibody Mab AG9 (200 ng/well) obtained according to a standard protocol and as previously described was added as a diluted solution in PBS buffer with 0.5% BSA and 0.1% of Polysorbate 20. After incubation for 1 h at 37 °C, the plate was washed four times with the TBS 80 buffer and a 3000 times diluted solution of IgG antimouse alkaline phosphatase (Promega, Leiden, The Netherlands) in the same buffer was added (100 μL/well). The wells were washed again four times and a revelation solution (150 μL/well) containing 5 mg of *para*-nitrophenyl phosphate in 5 mL of diethanolamine buffer was added for 30 min at room temperature. The reaction was stopped with 60 μL/well of 3 N NaOH solution. The measurement of the absorbance was performed at 405 nm with a background correction at 655 nm with a Bio-Rad photometer for a 96-well plate (Bio-Rad laboratories, CA, USA). Results were expressed as IC_{50}.[30]

Transient State Kinetics. Material. Highly purified myeloperoxidase of a purity index (A_{430}/A_{280}) of a least 0.86 was purchased from Planta Natural Products (http://www.planta.at). Its concentration was calculated using ε_{430} = 91 mM^{-1} cm^{-1}. Hydrogen peroxide, obtained from a 30% solution was diluted and the concentration determined by absorbance measurement at 240 nm where the extinction coefficient is 39.4 M^{-1} cm^{-1}. Tryptamine derivative stock solutions were prepared in dimethylsulfoxide (DMSO) and stored in dark flasks. Dilution was performed with 200 mM phosphate buffer, pH 7.4, to a final DMF concentration of 2% ($^v/_v$) in all assays.

Transient-State Kinetics. The multimixing stopped-flow measurements were performed with the Applied Photophysics (UK) instrument SX-18MV. When 100 μL were shot into a flow cell having a 1 cm light path, the fastest time for mixing two solutions and recording the first data point was 1.3 ms. Kinetics were followed both at single wavelength and by using a diode-array detector. At least three determinations (2000 data points) of pseudo-first-order rate constants (k_{obs}) were performed for each substrate concentration (pH 7.4, 25 °C) and the mean value was used in the calculation of the second-order rate constants, which were calculated from the slope of the line defined by a plot of k_{obs} versus substrate concentration. To allow calculation of pseudo-first-order rates, the concentrations of substrates were at least 5 times in excess of the enzyme.

Compound I and II Formation. Conditions of MPO Compound I formation were described recently.[59] Typically, 8 μM MPO were premixed with 80 μM H_2O_2, and after a delay time of 20 ms, Compound I was allowed to react with varying concentrations of tryptamine derivative in 200 mM phosphate buffer, pH 7.4. The reactions were followed at the Soret maximum of Compound II (456 nm). Compound II formation and reduction could be followed in one measurement. The resulting biphasic curves at 456 nm showed the initial formation of Compound II and its subsequent reduction to native MPO by the tryptamine derivatives (decrease in absorbance at 456 nm).

Acknowledgment. This study was supported by grants from the Belgian Fund for Scientific Research (FRS-FNRS), no. 34553.08, a grant from the FER 2007 (ULB) and a grant from the Department of International Relationship (BRIC

2007). We thank Prof. M. Luhmer and Dr. R. D'Orazio from CIREM (ULB) for NMR spectra recording.

Supporting Information Available: synthetic procedures not described in the Experimental Section, spectral analyses of the compounds, purity data of the final compounds, table of inhibition of the oxidation of LDL at three concentrations (1000, 100, and 50 nM). This material is available free of charge via the Internet at http://pubs.acs.org.

References

(1) Klebanoff, S. J. Myeloperoxidase: Friend and foe. *J. Leukocyte Biol*. **2005**, *77*, 598–562.
(2) Nicholls, S. J.; Hazen, S. L. Myeloperoxidase and cardiovascular disease. *Arterioscler. Thromb. Vasc. Biol*. **2005**, *25*, 1102–1111.
(3) Nicholls, S. J.; Hazen, S. L. Myeloperoxidase, modified lipoproteins, and atherogenesis. *J. Lipid Res*. **2009**, No. Suppl., S346–S351.
(4) Green, P. S.; Mendez, A. J.; Jacob, J. S.; Crowley, J. R.; Growdon, W.; Hyman, B. T.; Heinecke, J. W. Neuronal expression of myeloperoxidase is increased in Alzheimer's disease. *J. Neurochem*. **2004**, *90*, 724–733.
(5) Maruyama, Y.; Lindholm, B.; Stenvinkel, P. Inflammation and oxidative stress in ESRD—the role of myeloperoxidase. *J. Nephrol*. **2004**, *17*, S72–S76.
(6) Kettle, A. J.; Chan, T.; Osberg, I.; Senthilmohan, R.; Chapman, A. L. P.; Mocatta, T. J.; Wagener, J. S. Myeloperoxidase and protein oxidation in the airways of young children with cystic fibrosis. *Am. J. Resp. Crit. Care Med*. **2004**, *170*, 1317–1323.
(7) Minohara, M.; Matsuoka, T.; Li, W.; Osoegawa, M.; Ishizu, T.; Ohyagi, Y.; Kira, J.-I. Upregulation of myeloperoxidase in patients with opticospinal multiple sclerosis: positive correlation with disease severity. *J. Neuroimmunol*. **2006**, *178*, 156–160.
(8) Taguchi, J.; Miyazaki, Y.; Tsutsumi, C.; Sawayama, Y.; Ando, K.; Tsushima, H.; Fukushima, T.; Hata, T.; Yoshida, S.; Kuriyama, K. Expression of the myeloperoxidase gene in AC133 positive leukemia cells relates to the prognosis of acute myeloid leukemia. *Leukocyte Res*. **2006**, *30*, 1105–1112.
(9) Lefkowitz, D. L.; Lefkowitz, S. S. Microglia and myeloperoxidase: a deadly partnership in neurodegenerative disease. *Free Radic. Biol. Med*. **2008**, *45*, 726–731.
(10) Gray, E.; Thomas, T. L.; Betmouni, S.; Scolding, N.; Love, S. Elevated myeloperoxidase activity in white matter in multiple sclerosis. *Neurosci. Lett*. **2008**, *444*, 195–198.
(11) Itabe, H. Oxidative modification of LDL: its pathological role in atherosclerosis. *Clinic. Rev. Allergy Immunol*. **2009**, *37*, 4–11.
(12) Zouaoui-Boudjeltia, K.; Legssyer, I.; Van Antwerpen, P.; Lema Kisoka, R.; Babar, S.; Moguilevsky, N.; Delree, P.; Ducobu, J.; Remacle, C.; Vanhaeverbeek, M.; Brohee, D. Triggering of inflammatory response by myeloperoxidase-oxidized LDL. *Biochem. Cell Biol*. **2006**, *84*, 805–812.
(13) Shao, B. H.; Cavigiolio, G.; Brot, N.; Oda, M. N.; Heinecke, J. W. Methionine oxidation impairs reverse cholesterol transport by apolipoprotein A-1. *Proc. Natl. Acad. Sci. U.S.A*. **2008**, *105*, 12224–12229.
(14) Chantepie, S.; Malle, E.; Sattler, W.; Chapman, M. J.; Kontush, A. Distinct HDL subclasses present similar intrinsic susceptibility to oxidation by HOCl. *Arch. Biochem. Biophys*. **2009**, *487*, 28–35.
(15) Malle, E.; Furtmüller, P. G.; Sattler, W.; Obinger, C. Myeloperoxidase: a target for new drug development? *Br. J. Pharmacol*. **2007**, *152*, 838–854.
(16) Van Antwerpen, P.; Prévost, M.; Zouaoui-Boudjeltia, K.; Babar, S.; Legssyer, I.; Moreau, P.; Moguilevsky, N.; Vanhaeverbeek, M.; Ducobu, J.; Nève, J.; Dufrasne, F. Conception of myeloperoxidase inhibitors derived from flufenamic acid by computational docking and structure modification. *Bioorg. Med. Chem*. **2008**, *16*, 1702–1720.
(17) Tiden, A.-K.; Weistrand, C. Preparation of 1-(2-hydroxyethyl)-2-thioxo-1,2,3,5-tetrahydropyrrolo[3,2-*d*]pyrimidin-4-one as a myeloperoxidase (MPO) inhibitor. PCT Int. Appl. WO2007142577, 2007.
(18) Tiden, A.-K. Preparation of 2-thioxanthines as myeloperoxidase (MPO) inhibitors. PCT Int. Appl. WO2007142576, 2007.
(19) Tiden, A.-K.; Viklund, J. Preparation of thioxanthines as inhibitors of myeloperoxidase (MPO). PCT Int. Appl. WO2007120098, 2007.
(20) Boegevig, A.; Lo-Alfredsson, Y.; Pivonka, D.; Tiden, A.-K. Preparation of pyrrolo[3,2-*d*]pyrimidin-4-one derivatives as MPO enzyme inhibitors. PCT Int. Appl. WO2006062465, 2006.
(21) Tiden, A.-K.; Turek, D.; Viklund, J. Preparation of triazole derivatives as myeloperoxidase inhibitors. PCT Int. Appl. WO2006046910, 2006.
(22) Soyer, Z.; Bas, M.; Pabuccuoglu, A.; Pabuccuoglu, V. Synthesis of some 2(3*H*)-benzoxazolone derivatives and their in vitro effects on human leukocyte myeloperoxidase activity. *Arch. Pharm*. **2005**, *338*, 405–410.
(23) Svensson, M.; Tiden, A.-K.; Turek, D. Preparation of [1,2,4]-triazole-3-thiones as inhibitors of myeloperoxidase for the treatment of neuroinflammatory disorders. PCT Int. Appl. WO2004096781, 2004.
(24) Hanson, S.; Nordvall, G.; Tiden, A.-K. Preparation of xanthinethione derivatives as myeloperoxidase inhibitors. PCT Int. Appl. WO2003089430, 2003.
(25) Tanimoto, T.; Tanaka, I.; Nakajima, M. New myeloperoxidase inhibitors and their manufacture with *Penicillium*. Jpn. Kokai Tokkyo Koho JP2001131133, 2001.
(26) McLean, D. B.; Thompson, D. D. Pharmaceutical compositions containing myeloperoxidase inhibitors. U.S. Pat. Appl. US5719190, 1998.
(27) Glasebrook, A. L. 2-Phenyl-3-azoylbenzothiophenes for inhibition of myeloperoxidase activity. Eur. Pat. Appl. EP664125, 1995.
(28) Egan, R. W.; Hagmann, W. K.; Gale, P. H. Naphthalenes as inhibitors of myeloperoxidase: direct and indirect mechanisms of inhibition. *Agents Actions* **1990**, *29*, 266–276.
(29) Van Antwerpen, P.; Dufrasne, F.; Lequeux, M.; Zouaoui-Boudjeltia, K.; Lessgyer, I.; Babar, S.; Moreau, P.; Moguilevsky, N.; Vanhaeverbeek, M.; Ducobu, J.; Nève, J. Inhibition of the myeloperoxidase chlorinating activity by nonsteroidal anti-inflammatory drug flufenamic acid and its 5-chloro-derivative directly interact with a recombinant human myeloperoxidase to inhibit the synthesis of hypochlorous acid. *Eur. J. Pharmacol*. **2007**, *570*, 235–243.
(30) Van Antwerpen, P.; Boudjeltia-Zouaoui, K.; Babar, S.; Legssyer, I.; Moreau, P.; Moguilevsky, N.; Vanhaeverbeek, M.; Ducobu, J.; Nève, J. Thiol-containing molecules interact with the myeloperoxidase/H_2O_2/chloride system to inhibit LDL oxidation. *Biochem. Biophys. Res. Commun*. **2005**, *337*, 82–88.
(31) Jantschko, W.; Furtmüller, G. P.; Zederbauer, M.; Neugschwandtner, K.; Lehner, I.; Jakopitsch, C.; Arnhold, J.; Obinger, C. Exploitation of the unusual thermodynamic properties of human myeloperoxidase in inhibitor design. *Biochem. Pharmacol*. **2005**, *69*, 1149–1157.
(32) Ximenes, V. F.; Paino, I. M. M.; de Faria-Oliveira, O. M. M.; da Fonseca, L. M.; Brunetti, I. L. Indole ring oxidation by activated leukocytes prevents the production of hypochlorous acid. *Braz. J. Med. Biol. Res*. **2005**, *38*, 1575–1583.
(33) Galijasevic, S.; Abdulhamid, I.; Abu-Soud, H. M. Melatonin Is a Potent Inhibitor for Myeloperoxidase. *Biochemistry* **2008**, *47* (8), 2668–2677.
(34) Lu, T.; Galijasevic, S.; Abdulhamid, I.; Abu-Soud, H. M . Analysis of the mechanism by which melatonin inhibits human eosinophil peroxidase. *Br. J. Pharmacol*. **2008**, *154* (6), 1308–1317.
(35) Adrien, B.; Carmela, G.; Sylvain, P.; Yann, D.; de Sousa, R. A.; Valery, L.; Thierry, C.; Frederi, D. C.; Isabelle, A.; Thierry, M. Discovery and Refinement of a New Structural Class of Potent Peptide Deformylase Inhibitors. *J. Med. Chem*. **2007**, *50*, 10–20.
(36) Nishimura, S. *Handbook of Heterogeneous Catalytic Hydrogenation for Organic Synthesis*; J. Wiley & Sons, Inc: New York, 2001; pp 290−301.
(37) Lindquist, C.; Ersoy, O.; Somfai, P. Parallel synthesis of an indol-based library via an iterative Mannich reaction sequence. *Tetrahedron* **2006**, *62*, 3439–3445.
(38) Campos, K.; Woo, J.; Lee, S.; Tillyer, R. A general synthesis of substituted indoles from cyclic enol ethers and enol lactones. *Org. Lett*. **2004**, *6*, 79–82.
(39) Dufrasne, F.; Nève, J. Synthesis of 1,2-diamino-1-phenylpropane diastereoisomers from u-*N*-trifluoroacetyl-2-amino-1-phenylpropan-1-ol. *Monatsh. Chem*. **2005**, *163*, 739–746.
(40) Stevenson, R.; Sant Milid, P.; Haider, R.; Hilmi, A.; Al Farham, E. Method for making substituted indole. PCT Int. Appl. WO9959970, 1999.
(41) Hatzenbuhler, N. T.; Evrard, D. A.; Mewshaw, R. E.; Zhou, D.; Shah, U. S.; Inghrim, J. A.; Lenicek, S. E.; Baudy, R. B.; Butera, J. A.; Sabb, A. L.; Failli, A. A.; Ramamoorthy, P. S. A preparation of 3-aminochroman and 2-aminotetralin derivatives, useful in the treatment of serotonin-mediated disorders. PCT Int. Appl. WO2005012291, 2005.
(42) Hall, H.; Gisler, M. A Simple Method for Converting Nitriles to Amides. Hydrolysis with potassium hydroxide in *tert*-butyl alcohol. *J. Org. Chem*. **1976**, *41*, 3769–3770.
(43) Mewshaw, R. E.; Zhou, D.; Zhou, P.; Shi, X.; Hornby, G.; Spangler, T.; Scerni, R.; Smith, D.; Schechter, L. E.; Andree, T. H. Studies toward the Discovery of the Next Generation of Antidepressants. 3. Dual 5-HT1A and Serotonin Transporter Affinity within a Class of *N*-Aryloxyethylindoleylalkylamines. *J. Med. Chem*. **2004**, *47*, 3823–3842.
(44) Di Deo, M.; Marcantoni, E.; Torregiani, E.; Bartoli, G.; Bellucci, M. C.; Bosco, M.; Sambri, L. A simple, efficient, and general method for the conversion of alcohols into alkyl iodides by a

$CeCl_3 \cdot 7H_2O$/NaI system in acetonitrile. *J. Org. Chem.* **2000**, *65*, 2830–2833.
(45) Van der Mee, L.; Helmich, F.; De Bruijn, R.; Vekemans, J. A. J. M.; Palmans, A. R. A.; Meijer, E. W. Investigation of Lipase-Catalyzed Ring-Opening Polymerizations of Lactones with Various Ring Sizes: Kinetic Evaluation. *Macromolecules* **2006**, *39*, 5021–5027.
(46) Van Antwerpen, P.; Moreau, P.; Zouaoui-Boudjeltia, K.; Babar, S.; Dufrasne, F.; Moguilevsky, N.; Vanhaeverbeek, M.; Ducobu, J.; Nève, J. Development and validation of screening procedure for the assessment of inhibition using a recombinant enzyme. *Talanta* **2007**, *75*, 503–510.
(47) Kettle, A. J.; Winterbourn, C. C. Superoxide modulates the activity of myeloperoxidase and optimizes the production of hypochlorous acid. *Biochem. J.* **1988**, *252*, 529–536.
(48) Carr, A. C.; Myzak, M. C.; Stocker, R.; McCall, M. R.; Frei, B. Myeloperoxidase binds to low-density lipoprotein: potential implications for atherosclerosis. *FEBS Lett.* **2000**, *487*, 176–180.
(49) Furtmüller, P. G.; Zederbauer, M.; Jantschko, W.; Helm, J.; Bogner, M.; Jakopitsch, C.; Obinger, C. Active site structure and catalytic mechanisms of human peroxidases. *Arch. Biochem. Biophys.* **2006**, *445*, 199–213.
(50) Blair-Johnson, M.; Fiedler, T.; Fenna, R. Human myeloperoxidase: structure of a cyanide complex and its interaction with bromide and thiocyanate substrates at 1.9 Å resolution. *Biochemistry* **2001**, *40*, 13990–13997.
(51) Sadowski, J.; Gasteiger, J. From atoms and bonds to three-dimensional atomic coordinates: automatic model builders. *Chem. Rev.* **1993**, *93*, 2567–2581.
(52) Friesner, R. A.; Banks, J. L.; Murphy, R. B.; Halgren, T. A.; Klicic, J. J.; Mainz, D. T.; Repasky, M. P.; Knoll, E. H.; Shelley, M.; Perry, J. K. Glide: a new approach for rapid, accurate docking and scoring. 1. Method and assessment of docking accuracy. *J. Med. Chem.* **2004**, *47*, 1739–1749.
(53) Shelley, J. C.; Cholleti, A.; Frye, L. L.; Greenwood, J. R.; Timlin, M. R.; Uchimaya, M. Epik: a software program for p*K*(a) prediction and protonation state generation for drug-like molecules. *J. Comput.-Aided Mol. Des.* **2007**, *21*, 681–691.
(54) Smid, P.; Coolen, H. K. A. C.; Keizer, H. G.; Van Hes, R.; De Moes, J.; Den Hartog, A. P.; Stork, B.; Plekkenpol, R. H.; Niemann, L. C.; Stroomer, C. N. J.; Tulp, M. Th. M.; Van Stuivenberg, H. H.; McCreary, A. C.; Hesselink, M. B.; Herremans, A. H. J.; Kruse, C. G. Synthesis, Structure−Activity Relationships, and Biological Properties of 1-Heteroaryl-4-[ω-(1*H*-indol-3-yl)alkyl]piperazines, Novel Potential Antipsychotics Combining Potent Dopamine D2 Receptor Antagonism with Potent Serotonin Reuptake Inhibition. *J. Med. Chem.* **2005**, *48*, 6855–6869.
(55) Mewshaw, R. E.; Zhou, D.; Zhou, P.; Shi, X.; Hornby, G.; Spangler, T.; Scerni, R.; Smith, D.; Schechter, L. E.; Andree, T. H. Studies toward the Discovery of the Next Generation of Antidepressants. 3. Dual 5-HT1A and Serotonin Transporter Affinity within a Class of *N*-Aryloxyethylindolylalkylamines. *J. Med. Chem.* **2004**, *47*, 3823–3842.
(56) Hewson, W. D.; Hager, L. P. Mechanism of the chlorination reaction catalyzed by horseradish peroxidase with chlorite. *J. Biol. Chem.* **1979**, *254*, 3175–3181.
(57) Havel, R. J.; Eder, H. A.; Bragdon, J. H. Distribution and chemical composition of ultracentrifugally separated lipoproteins in human serum. *J. Clin. Invest.* **1955**, *34*, 1345–1353.
(58) Moguilevsky, N.; Zouaoui-Boudjeltia, Z.; Babar, S.; Delrée, P.; Legssyer, I.; Carpentier, Y.; Vanhaeverbeek, M.; Ducobu, J. Monoclonal antibodies against LDL progressively oxidized by myeloperoxidase react with ApoB-100 protein moiety and human atherosclerotic lesions. *Biochem. Biophys. Res. Commun.* **2004**, *323*, 1223–1228.
(59) Furtmüller, P. G.; Burner, U.; Obinger, C. Reaction of human myeloperoxidase Compound I with chloride, bromide, iodide, and thiocyanate. *Biochemistry* **1998**, *37*, 17923–17930.